



HAL
open science

Wind power predictions from nowcasts to 4-hour forecasts: a learning approach with variable selection

Dimitri Bouche, Rémi Flamary, Florence D'alché-Buc, Riwal Plougonven,
Marianne Clausel, Jordi Badosa, Philippe Drobinski

► To cite this version:

Dimitri Bouche, Rémi Flamary, Florence D'alché-Buc, Riwal Plougonven, Marianne Clausel, et al..
Wind power predictions from nowcasts to 4-hour forecasts: a learning approach with variable selection.
Renewable Energy, 2023, 211, pp.938-947. 10.1016/j.renene.2023.05.005 . hal-04254953

HAL Id: hal-04254953

<https://hal.science/hal-04254953v1>

Submitted on 23 Oct 2023

HAL is a multi-disciplinary open access archive for the deposit and dissemination of scientific research documents, whether they are published or not. The documents may come from teaching and research institutions in France or abroad, or from public or private research centers.

L'archive ouverte pluridisciplinaire **HAL**, est destinée au dépôt et à la diffusion de documents scientifiques de niveau recherche, publiés ou non, émanant des établissements d'enseignement et de recherche français ou étrangers, des laboratoires publics ou privés.

Wind power predictions from nowcasts to 4-hour forecasts: a learning approach with variable selection

Dimitri Bouche^{a*}, Rémi Flamary^d, Florence d’Alché-Buc^a, Riwal Plougonven^b,
Marianne Clausel^c, Jordi Badosa^b, Philippe Drobinski^b

Abstract

We study short-term prediction of wind speed and wind power (every 10 minutes up to 4 hours ahead). Accurate forecasts for these quantities are crucial to mitigate the negative effects of wind farms’ intermittent production on energy systems and markets. We use machine learning to combine outputs from numerical weather prediction models with local observations. The former provide valuable information on higher scales dynamics while the latter gives the model fresher and location-specific data. So as to make the results usable for practitioners, we focus on well-known methods which can handle a high volume of data. We study first variable selection using both a linear technique and a nonlinear one. Then we exploit these results to forecast wind speed and wind power still with an emphasis on linear models versus nonlinear ones. For the wind power prediction, we also compare the indirect approach (wind speed predictions passed through a power curve) and the indirect one (directly predict wind power).

Keywords—Wind speed forecasting, Wind energy forecasting, Machine learning, Numerical weather prediction, Downscaling

Abbreviations—Numerical weather prediction (NWP); machine learning (ML); European Centre for Medium-Range Weather Forecasts (ECMWF); parc de Bonneval (BO); parc de Moulin de Pierre (MP); parc de Beaumont (BM); parc de la Renardière (RE); parc de la Vènerie (VE); kernel ridge regression (KRR); neural network (NN); ordinary least squares (OLS); forward stepwise ordinary least square (OLS f-stepwise); reproducing kernel Hilbert space (RKHS); Hilbert-Schmidt independence criterion (HSIC); Backward selection with HSIC (BAHSIC); normalized root mean squared error (NRMSE)

1 Introduction

The fast development of renewable energies is a necessity to mitigate climate changes [22]. Wind energy has developed rapidly over the past three decades, with an average annual growth rate of 23.6% between 1990 and 2016 [17], and is now considered as a mature technology. The share of renewable energies in global electricity generation reached 29% in 2020, and is expected to keep growing fast in coming years [18] which raises a number of challenges, stemming from the variability and spatial distribution of the resource. Then, in order to facilitate the dynamic management of electricity networks, forecasts of wind energy require continual improvement. Short timescales, from a few minutes to a few hours, are of particular importance for operations.

To produce forecasts, one can rely on several distinct sources of information. On timescales of half a day to about a week, deterministic weather forecasts provide a representation on a grid of the atmospheric state, including wind speed near the surface. The skill of such numerical weather forecasts (NWP) models has continually increased over the past decades [2], while their spatial resolution has also grown finer (down to few km). However, to predict at a given geographical location for time horizons shorter than a day, the use NWP models is impeded by two main

^a LTCI, Télécom Paris, Institut Polytechnique de Paris

^b LMD-IPSL, Ecole polytechnique - IP Paris, ENS - PSL Université, Sorbonne Université, CNRS, France

^c Université de Lorraine, CNRS, IECL

^d CMAP, Ecole Polytechnique, Institut Polytechnique de Paris

* **Corresponding author:** dimi.bouche@gmail.com

difficulties being (i) the errors in the modeled wind and (ii) the relatively infrequent initiation of forecasts. The former result from both limited resolution and the impossibility to model local processes. For instance, for wind speed at an altitude of 100m is strongly affected by local small-scale features and turbulent motions, both of which remain beyond the spatial resolution that is achievable for NWP models. Regarding the second point, operational centers typically launch forecasts twice or four times per day, however the computation of the forecast itself as well as the preparation of its initial state require time and computational resources—see e.g. [19]. As a result, many methodologies for forecasting short-term wind speed or wind power use only past local observations and focus on statistical methods—see e.g. the reviews from Tascikaraoglu and Uzunoglu [29], Okumus and Dinler [23], Liu et al. [21] and references therein. Nevertheless, we know that NWP models can provide valuable information for the evolution of the atmosphere on larger scales—i.e. on the formation or passage of a low-pressure system and on the associated fronts.

It is therefore a natural idea to use both sources of information to train machine learning (ML) models: local deficiencies in NWP models can partly be overcome by *downscaling*; i.e. better estimating local variables from the knowledge from a model’s outputs and past observations. Such efforts have been carried out for decades in meteorology and climatology, under different names. In a pioneering early study, [9] applied multilinear regressions trained on past observations to correct NWP errors. More recently, *model output statistics* has become common practice in operational weather forecast centers (see e.g. [32, 1]). In recent years, ML methods have enhanced the performance of these post-processing steps (see e.g. [34, 10]).

Specifically for wind speed or wind power forecasting, several *hybrid models* combining successfully NWP outputs with local observations have been proposed. In terms of time horizons, the focus is mostly on forecasts beyond 1 hour with low resolution (generally one prediction per hour)—see e.g. Hoolohan et al. [16, Table 1] and references therein. While for the shorter term, most existing hybrid methods rely on complex and deep architectures—see e.g. Han et al. [14, Table 1] and references therein. Moreover, for all these methods only a very low number of local and NWP variables are used (most of the times, only the past observed wind speeds and the ones predicted by the NWP model).

In this paper, we study hybrid prediction of both wind speed and wind power. Our contributions are five-fold.

- We study the problem for time horizons ranging from 10 minutes to 4 hours at a high resolution (every 10 minutes). This allows us to study with precision when and how the transition from one source of information (past local observations) to the other (NWP forecasts) occurs. This setting has been introduced in Dupré et al. [6] yet we extend it and use it to address the following new problems.
- We include many different outputs from a NWP model as they could provide broader information on the overall predicted dynamics to the ML model. We also include several local variables. We then focus on variable selection and study the evolution of the importance of the selected variables through time. This allows us to better understand the nature of the studied statistical relationship and to extract a usable set of relevant variables.
- We study five distinct wind farms which enables us to expose many similarities but also some site specificities and increases the statistical significance of our results.
- We investigate which type of ML methods are the most suited for hybrid prediction of wind speed and wind power.
- Many existing contribution focus either on wind power or wind speed prediction but not on the relation between them, whereas at all steps of the paper, we compare the direct (predict wind power) and indirect (wind speed predictions passed through a power curve) approaches.

In terms of methodology, we have two key focuses.

- We want this study to be usable by practitioners. To that end we concentrate on a reduced choice of well-known and efficient ML methods which scale well with the number of samples, and moreover provide all the needed elements for a straightforward implementation. We also put a particular emphasis on how we select our models.
- We want to ensure our results are statistically significant. To that end, we employ a thorough evaluation process. We study several sites over several periods of time (the number of samples is quite high per site) and for each location, we average the results over several data splits.

In Section 2, we introduce the data set from Zéphyr ENR and detail our processing of the data. Section 3 is dedicated to the presentation of our methodology as well as to the introduction of the statistical learning tools. Then in Section 4 investigates variable selection. Finally in Section 5,



Figure 1: Cartography of the studied farms, BM (A), BO (B), MP (C), RE (D), VE (E)

exploiting all the previous results, we compare different well-known ML models as well as direct and indirect prediction for wind power.

Notation We introduce the following notation: for two integers $n_0, n_1 \in \mathbb{N}^*$, the set of strictly positive integers, we denote by $\llbracket n_0 \rrbracket$ the set $\{1, \dots, n_0\}$ and by $\llbracket n_0, n_1 \rrbracket$ the set $\{n_0, \dots, n_1\}$.

2 Data and context

In this Section, we introduce the dataset that we use (Section 2.1) as well as the pre-processing steps that we apply to it and the general evaluation methodology (Section 2.2).

2.1 Zéphyr ENR’s dataset

Variable type	Altitude or pressure level	Variable	Unit	
Surface	10m/100m	Zonal wind speed	ms^{-1}	
		Meridional wind speed	ms^{-1}	
	2m	Temperature	K	
		Dew point temperature	K	
		Surface pressure	Pa	
	Surface		Skin temperature	K
			Mean sea level pressure	Pa
			Surface latent heat flux	Jm^{-2}
			Surface sensible heat flux	Jm^{-2}
			Boundary layer dissipation	Jm^{-2}
			Boundary layer height	m
Altitude	1000/925/850/700/500	Zonal wind speed	ms^{-1}	
		Meridional wind speed	ms^{-1}	
		Geopotential height	m^2s^{-2}	
		Divergence	s^{-1}	
		Vorticity	s^{-1}	
		Temperature	K	
Computed	10m/100m	Norm of wind speed	ms^{-1}	
	10m to 925 hPa	Wind shear	ms^{-1}	
		Temperature gradient	K	

Table 1: ECMWF variables

Availability	Variable	Unit
All	Wind speed	ms ⁻¹
All	Power output	kW
All	Wind direction	Degree
BO and BM	Temperature	Celsius degree

Table 2: In situ variables

Variable (source)	Abbreviation
Wind speed (in situ)	WS
Power output (in situ)	PW
Norm of wind speed at 100m (ECMWF)	F10
Norm of wind speed at 100m (ECMWF)	F100
Wind shear between 10m and 925 hPa (ECMWF)	DF
Boundary layer dissipation (ECMWF)	bld
Boundary layer height (ECMWF)	blh
Surface latent heat flux (ECMWF)	slhf

Table 3: Abbreviations for the variables used in the paper

Our first source of information consists of measurements made by sensors in the wind turbines (we call these in situ variables) whereas the second one consists of forecasts from the European Centre for Medium-Range Weather Forecasts (ECMWF). We study five wind farms in the northern half of France: Parc de Bonneval (BO), Moulin de Pierre (MP), Parc de Beaumont (BM), Parc de la Renardière (RE), and Parc de la Vènerie (VE). These wind farms are operated by the private company Zéphyr ENR and are described in details in [7]. We display their location on a map in Figure 1. Some are geographically close by—we can form the pairs (BO, MP) and (BM, RE)—while VE is isolated. Note that we left another available farm out of the study because it displayed signs of sensors deficiencies. On the one hand, the geographical topology of the surroundings for (BO, MP) and (BM, RE) are quite similar, they correspond to open fields with very few elevation variations. On the other hand, VE is surrounded by wooded countryside with slightly more elevation variations, which may explain the differences that we observe between this farm and the others in Sections 4 and 5.

For BO and VE we have three years of data (from 2015 to 2017) which amounts to a total of $n = 157680$ observations for BO. However, for VE we do not use the year 2016 because it encompasses sensor deficiencies, so we use $n = 105120$ observations. For BM and RE we have access to two years of data (from 2017 to 2018 for BM and from 2015 to 2016 for RE) which results in a total of $n = 105120$ observations, and finally for MP we have only one year (2017), which gives us of total of $n = 52560$ observations.

Several variables are available, we summarize the in situ ones in Table 2—note the temperature is available only for BO and BM. In order to encode the circular nature of the in situ wind direction we encode it using two trigonometric variables.

The ECMWF provides global forecasts issued by their NWP models. We followed [6]: we extracted the day ahead forecast twice a day (at 0000UTC and 1200UTC) and included the same 47 variables as they do. These variables are either selected or computed so as to describe as well as possible the boundary layer, the wind parameters and the temperature in the lower troposphere. Table 1 presents the ECMWF variables we use. They can be either surface variables, altitude ones, or computed from other ECMWF variables. The spatial resolution of ECMWF forecasts is about 16 km (0.125° in latitude and longitude) and their temporal resolution is 1h, then to match that of the in situ variables (10 min), we linearly interpolate the ECMWF forecasts. To finish with we sum up the abbreviations for the variables mostly used in the paper in Table 3.

2.2 Preprocessing and evaluation methodology

In order to increase the statistical significance of our results, we average the outcomes of the experiments over different data splits. A split consists of 3 subsets from the dataset, a train subset (of size n_{train}), a validation one (size n_{val}) and a test one (of size n_{test}). In order to avoid overfitting, given a ML method and a set of possible parameter values, we first train the resulting models on the train set. Then we choose the model yielding the best score on the validation set. To finish with, we re-train this model on the concatenation of the train and validation set and report its score on

the test set. So as to preserve time coherence, we build our splits in a rolling fashion. For instance for the first split we take the period $\llbracket n_{\text{train}} \rrbracket$ for training, the period $\llbracket n_{\text{train}} + 1, n_{\text{train}} + n_{\text{val}} \rrbracket$ for validation and we test the models on the period $\llbracket n_{\text{train}} + n_{\text{val}} + 1, n_{\text{train}} + n_{\text{val}} + n_{\text{test}} \rrbracket$. Then for the second split, the train period is $\llbracket n_{\text{train}} + n_{\text{val}} + n_{\text{test}} + 1, 2n_{\text{train}} + n_{\text{val}} + n_{\text{test}} \rrbracket$, the validation one is $\llbracket 2n_{\text{train}} + n_{\text{val}} + n_{\text{test}} + 1, 2n_{\text{train}} + 2n_{\text{val}} + n_{\text{test}} \rrbracket$ and so on. For the sizes of the windows, we set $n_{\text{train}} = 10000$, $n_{\text{val}} = 10000$ and $n_{\text{test}} = 10000$ (however, the last split generally contains around $5000 \leq n_{\text{test}} \leq 10000$ observations). Since the length of available data vary from farm to farm, we do not have the same number of splits for all the farms.

We pre-process the data in the following way. As the number of wind turbines per farm is quite low (6 for BM, 6 for BO, 3 for HC, 6 for MP, 6 for RE and 4 for VE) , we average the in situ data over the turbines for each farm. In all our experiments, we standardize both the input and the output variables (subtract the mean and divide by the standard deviation) using the training data. We do so both for in situ variables and ECMWF ones. Such operation is crucial for instance to avoid favoring some variables which are structurally bigger over others when using regularized ML models.

3 Methodology and machine learning tools

In this Section, we introduce our general methodology as well as the ML tools that we use for variable selection and forecasting.

3.1 Methodology

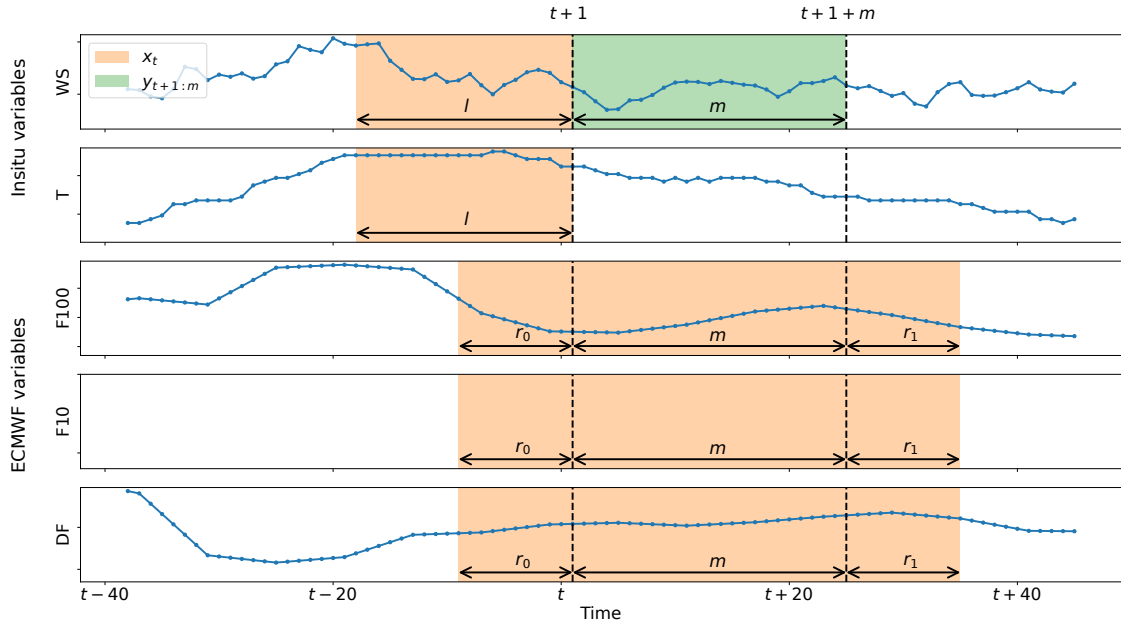


Figure 2: Summary of the time windows used for each source of data for wind speed prediction

Dataset building. Let $m \in \mathbb{N}$ be the prediction length (the number of future wind speed or wind power values we want to forecast). For the ECMWF variables, we include the corresponding forecasts. However, in practice we found that including a bit more than that improved performances. To that end, we denote respectively by $r_0 \in \mathbb{N}$ the number of past ECMWF predictions that we include, and by $r_1 \in \mathbb{N}$ the number of ECMWF predictions that we consider after m . For the in situ variables, we include a length $l \in \mathbb{N}$ of past observations. These different time windows are illustrated in Figure 3.1 for a reduced set of variables. For the all the variables and time windows, we concatenate the relevant observations \mathbf{x}_t (these within the orange zones in Figure 3.1). From these, we want to produce a prediction for $\mathbf{y}_{t+1:m} \in \mathbb{R}^m$ (the m observations within the green zone in Figure 3.1). In practice, we use the following parameters which work well experimentally:

- we predict up to 4 hours, with a time sampling rate of 10 min, it means that $m = \frac{4 \times 60}{10} = 24$,
- for the in situ variables, we consider 3h of past observations, thus $l = \frac{3 \times 60}{10} = 18$,

- for the ECMWF variables we additionally use the predictions between 1.5h before and 1.5h after the time horizon of interest so $r_0 = r_1 = \frac{1.5 \times 60}{10}$.

ML models. We stick to ML models which are well-known and can scale well to a higher volume of data. Good results were obtained for one location (BO) from the studied dataset in Dupré et al. [6] using linear regression with greedy forward stepwise variable selection [15]. Nevertheless, since we are interested in the importance of variables, we study also an alternative which select variables directly in the least square problem. The LASSO [30] exploits the L1 penalty to induce sparsity in the regression coefficients, thus shrinking to zero the ones which are associated to the less relevant variables. Such methods can however be limited in that they can learn only linear dependencies between the input and output variables. Consequently, we study a nonlinear alternative: kernel ridge regression (KRR)—see for instance [26, 27]. Finally, in order to include most families of ML models, we consider two other nonlinear methods: a tree-based boosting algorithm [8] (we use XG-Boost Chen and Guestrin [4]) as well as a feed-forward neural network (NN). In Section 3.2 we give more mathematical details on the general ML problem as well as on the methods that perform the best in the experimental section.

Variable selection. We have many in situ and ECMWF variables available (see Tables 1 and 2). So as to improve the computational efficiency and understand better what the models do, it is preferable to use only the most important variables. Ideally, we want to find a subset which is sufficient for a model to predict a statistically relevant target value from the input variables. In that sense a variable selection tool is necessarily model specific. Linear techniques will focus only on linear dependencies, whereas nonlinear ones will incorporate a much wider range of dependencies. Then we propose to use and interpret the results of one variable selection for each type. For the linear one we study the LASSO. For the nonlinear one, we use backward elimination using the Hilbert Schmidt Independence Criterion [28]. As opposed to the LASSO, it performs variable selection as an independent first step. The selected variables can then be used downstream to train any model. Then, for the nonlinear models (KRR, XG-Boost, feed-forward NN), we use the variables selected through this method. We give more detailed insights into the different techniques in Section 3.3.

3.2 Details on machine learning models

The input observations are the concatenation of the different variables on the time windows described in the previous section. We denote by $\mathcal{X} = \mathbb{R}^q$ the resulting input space, for some $q \in \mathbb{N}$. Our training data then consist of $((\mathbf{x}_t, \mathbf{y}_{t+1:m}))_{t=1}^n \in (\mathcal{X} \times \mathbb{R}^m)^n$ for some $n \in \mathbb{N}$, where we recall that $\mathbf{y}_{t+1:m} = (y_{t+1+m_0})_{m_0=1}^m$. Given a prediction function from a ML model class $f_{\mathbf{w}} : \mathcal{X} \rightarrow \mathcal{Y}$ parameterized by a vector $\mathbf{w} \in \mathcal{W}$, we want to minimize the average error on the training data:

$$\min_{\mathbf{w} \in \mathcal{W}} \frac{1}{n} \sum_{t=1}^n \|f_{\mathbf{w}}(\mathbf{x}_t) - \mathbf{y}_{t+1:m}\|_2^2 + \lambda \Omega(\mathbf{w}). \quad (1)$$

However, depending on the model, a penalty function $\Omega : \mathcal{W} \rightarrow \mathbb{R}$ can be added in order to prevent overfitting or promote variable selection; its intensity is controlled by a parameter $\lambda > 0$.

In practice, instead of predicting all time horizons in one go as in Problem (1), we rather use separate models for each horizon in $\llbracket t+1, t+1+m \rrbracket$. That way we can tailor the different parameters for each horizon, which we found improved performances. Then in what follows, we consider a generic time horizon m and predict y_{t+1+m} .

Ordinary least squares (OLS). In forward stepwise variable selection [15], at each step an OLS regression is solved for which the optimization problem reads:

$$\min_{\mathbf{w} \in \mathcal{W}, b \in \mathbb{R}} \frac{1}{n} \sum_{t=1}^n (\mathbf{w}^T \mathbf{x}_t + b - y_{t+1+m})^2 \quad (2)$$

A well-known and simple closed form exist, which we use in practice.

LASSO. The optimization problem for the LASSO is the following:

$$\min_{\mathbf{w} \in \mathcal{W}, b \in \mathbb{R}} \frac{1}{n} \sum_{t=1}^n (\mathbf{w}^T \mathbf{x}_t + b - y_{t+1+m})^2 + \lambda \|\mathbf{w}\|_1,$$

where $\|\mathbf{w}\|_1$ is the sum of the absolute values of the coefficients \mathbf{w} . Many efficient algorithms exist to solve this convex yet non differentiable problem—see for instance [3]. In practice we use the scikit-learn [24] implementation with coordinate descent solver.

Kernel ridge regression (KRR). In KRR, we consider a class of models defined by a positive definite reproducing kernel $k : \mathcal{X} \times \mathcal{X} \rightarrow \mathbb{R}$ which results in a unique associated reproducing kernel Hilbert space (RKHS). A most typical choice for k is the Gaussian kernel:

$$k_\gamma(\mathbf{x}, \mathbf{x}') := \exp(-\gamma(\|\mathbf{x} - \mathbf{x}'\|_2^2)).$$

We then seek our modeling function in this RKHS which we denote \mathcal{H}_k , each $h \in \mathcal{H}_k$ being a function from \mathcal{X} to \mathbb{R} . For many kernels, this space constitutes a very rich class of modeling functions which can model nonlinear dependencies. The optimization problem reads:

$$\min_{h \in \mathcal{H}_k} \frac{1}{n} \sum_{t=1}^n (h(\mathbf{x}_t) - y_{t+1+m})^2 + \lambda \|h\|_{\mathcal{H}_k}^2 \quad (3)$$

where $\|\cdot\|_{\mathcal{H}_k}^2$ is the RKHS norm on \mathcal{H}_k , which measure in a sense the smoothness of functions in \mathcal{H}_k . Thanks to the Representer theorem, any solution to Problem (3) can be parameterized by a vector $\boldsymbol{\alpha} \in \mathbb{R}^n$:

$$h_{\boldsymbol{\alpha}} := \sum_{j=1}^n \alpha_j k(\mathbf{x}_j, \cdot),$$

which makes optimization in the RKHS amenable. For KRR the optimal coefficients $\hat{\boldsymbol{\alpha}}$ can be found in close form:

$$\hat{\boldsymbol{\alpha}} := (K + n\lambda I)^{-1} \mathbf{y}^{(m)},$$

with $\mathbf{y}^{(m)} := (y_{t+1+m})_{t=1}^n$, $I \in \mathbb{R}^{n \times n}$ the identity matrix and $K \in \mathbb{R}^{n \times n}$ with entries $K_{tj} = k(\mathbf{x}_t, \mathbf{x}_j)$.

In practice, to handle the large volume of training data, we use an approximated version of KRR. Nyström approximation [31, 5] exploits a random subset of points from the training data. Concretely, we sample randomly and uniformly without replacement $p \in \mathbb{N}$ indices $\{i_1, \dots, i_p\}$ among the integers in $\llbracket n \rrbracket$, and replace $h_{\hat{\boldsymbol{\alpha}}}$ —see e.g. [25]—with:

$$\tilde{h}_{\tilde{\boldsymbol{\alpha}}} := \sum_{j=1}^p \tilde{\alpha}_j k(\mathbf{x}_{i_j}, \cdot),$$

where $\tilde{\boldsymbol{\alpha}} \in \mathbb{R}^p$ is given by the following close form:

$$\tilde{\boldsymbol{\alpha}} := (K_{np}^T K_{np} + \lambda n K_{pp})^\dagger K_{np}^T \mathbf{y}^{(m)}. \quad (4)$$

Where A^\dagger denotes the Moore-Penrose pseudo-inverse of a matrix A , and $K_{np} \in \mathbb{R}^{n \times p}$ is defined by the entries $(K_{np})_{tj} := k(\mathbf{x}_t, \mathbf{x}_{i_j})$ and $K_{pp} \in \mathbb{R}^{p \times p}$ by the entries $(K_{pp})_{bj} = k(\mathbf{x}_{i_b}, \mathbf{x}_{i_j})$.

3.3 Details on variable selection

OLS with forward stepwise selection (OLS f-stepwise). When performing linear regression, variable selection can be performed in a greedy manner. First an intercept is fit to the data and then at each step we solve OLS problems—Problem (2)—adding in turns each one of the remaining variables. We then keep the one which best improve the model according to some criterion. In [6], the Bayesian information criterion is used. However, in our experiments we rather used the improvement of the score on half of the validation set, as it led to better experimental performances.

LASSO. Provided the regularization intensity λ is well chosen, the L1 penalty of the LASSO shrinks the coefficients associated the variables which are less important towards zero. Then the model uses mostly the relevant variables and the magnitude of the coefficients can be looked at to deduce what these variables are. This is the type of analysis that we perform in Section 4.1.

Hilbert-Schmidt independence criterion (HSIC). The HSIC [12] is an independence measure. Similarly to the KRR, it makes use of RKHSs to embed implicitly a set of observations into a high-dimensional space and consider a notion of independence in this space which allows for detection of nonlinear dependencies. More precisely, let us consider a positive-definite kernel $k : \mathcal{X}^2 \rightarrow \mathbb{R}$ for the input observations and a one $g : (\mathbb{R}^m)^2 \rightarrow \mathbb{R}$ for the output observations. For this variable selection technique, we consider all time horizons in $\llbracket t+1, t+1+m \rrbracket$ together as the kernelized framework allows for this. In practice, we estimate HSIC from the data as [13]:

$$\widehat{\text{HSIC}} := \frac{1}{n^2} \text{Trace}(HKG),$$

where $H \in \mathbb{R}^{n \times n}$ is the centering matrix $H := \frac{1}{n}(I - \mathbf{1}\mathbf{1}^T)$ with $\mathbf{1} \in \mathbb{R}^n$ a vector full of ones and $I \in \mathbb{R}^{n \times n}$ the identity matrix. The matrices $K \in \mathbb{R}^{n \times n}$ and $G \in \mathbb{R}^{n \times n}$ are the kernel matrices:

$$\begin{aligned} (K)_{tj} &:= k(\mathbf{x}_t, \mathbf{x}_j), \\ (G)_{tj} &:= g(\mathbf{y}_{t+1:m}, \mathbf{y}_{j+1:m}). \end{aligned}$$

HSIC takes its values between 0 and 1, a value of 0 meaning independence and a value of 1 means full dependence.

However, to be able to compute the estimator for the large number of data points, we recourse to Nyström approximation as well [35]. We then sample randomly and uniformly without replacement $p \in \mathbb{N}$ indices $\{i_1, \dots, i_p\}$ from the integers in $\llbracket n \rrbracket$ for the input observations and $p' \in \mathbb{N}$ ones $\{i'_1, \dots, i'_{p'}\}$ for the output observations. We then define the Nyström features maps [33] (centered in the feature space using H):

$$\begin{aligned} \widehat{\Phi} &:= HK_{np}K_{pp}^{-\frac{1}{2}}, \\ \widehat{\Psi} &:= HG_{np'}G_{p'p'}^{-\frac{1}{2}}, \end{aligned}$$

where the matrices K_{np} and K_{pp} are defined as for Equation (4) and the matrices $G_{np'}$ and $G_{p'p'}$ are defined similarly for the kernel g however based on the set of indices $\{i'_1, \dots, i'_{p'}\}$. The Nyström HSIC estimator is then [35]:

$$\widehat{\text{HSIC}} := \left\| \frac{1}{n} \widehat{\Phi}^T \widehat{\Psi} \right\|_F^2,$$

where for a matrix A , the Frobenius norm is defined as $\|A\|_F^2 := \text{Trace}(A^T A)$.

Backward selection with HSIC (BAHSIC). To perform variable selection, we start with all the available variables and then at each round, we compute the HSICs between the input variables and the target variable removing one input variable at a time. A given percentage of the input variables for which these HSICs are the highest are removed. We keep iterating in this way to rank the variables. Then, the ones removed the latest are the most important ones. The detailed algorithm corresponds to Algorithm 1 in [28]. A forward version exists as well, however, the authors advocate the use of backward selection to avoid missing important variables. Finally as a side note, in practice we use as Gaussian kernels setting bandwidth following the recommendations from [28].

4 Importance of variables and their evolution through time

In this section, we study variable selection using the LASSO in Section 4.1 and BAHSIC in Section 4.2 to determine which variables are the most important and how their importance evolves through time.

4.1 Linear variable selection with LASSO

LASSO scores. We now describe the computations carried out to extract a subset of relevant variables suitable for interpretation from fitted LASSO models. In practice for each data split, we validated the regularization parameter λ on the validation set and obtained estimated LASSO coefficients. Now to reduce the number of variables we must rank them according to an importance metric based on these coefficients; we do so for each time horizon separately. So as to avoid assigning more weight to models for which λ was selected small, for each farm and each data split we normalize the coefficients by the absolute value of the biggest one. As opposed to the grouped variable selection performed in Section 4.2, the observations through time for a given variable can be separated by the LASSO shrinking (a variable can be selected for instance at time t_0 but not at t_1). Consequently, we sum the normalized coefficients corresponding to different time instants for the same variable and in doing so, we obtain a single quantity per variable. Then we average these quantities over the data splits and call the resulting quantities LASSO scores. To sum up, at this point we have for each prediction horizon and each farm a set of such scores for each variable. Then, to select variables, we average these LASSO scores over farms. Finally, based on these

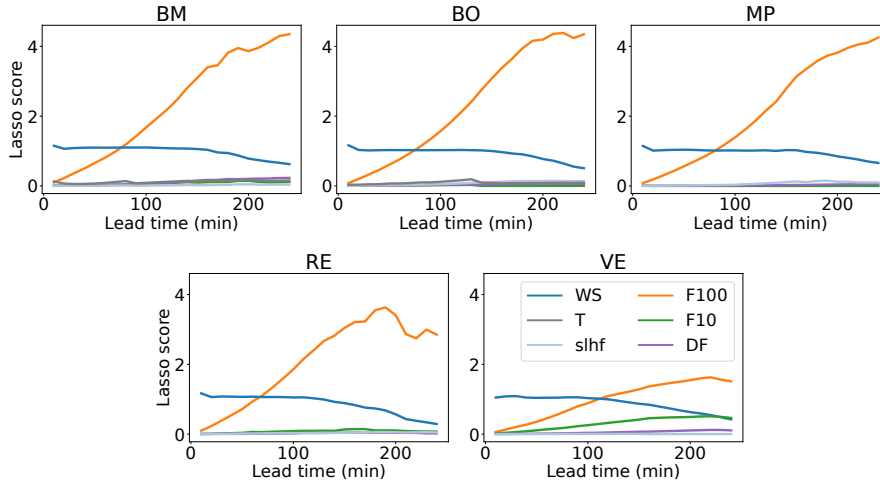


Figure 3: Linear variable selection with the LASSO (Wind speed as target)

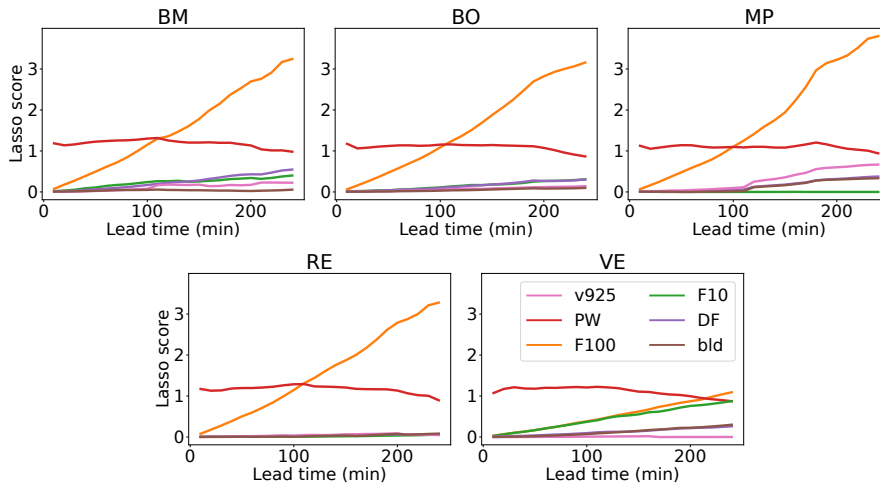


Figure 4: Linear variable selection with the LASSO (Wind power as target)

average scores, for each prediction horizon, we keep the top 6 variables.

Interpretation. For these selected variables, we plot the evolution through time of the LASSO scores in Figure 3 for wind speed and in Figure 4 for wind power. We make the following key observations:

- At all locations, two variables are much more important than the rest. The in situ observed wind speeds (WS) and the ECMWF predicted wind speed at altitude 100m (F100) stand out for wind speed prediction. For wind power prediction, the in situ power production (PW) along with F100 are of particular importance. We can relate these results to the good performances of the LASSO for wind speed prediction in Section 5. Then if we look at the relative magnitudes of the coefficients, we can deduce that only using a linear combination of past local wind speeds (WS) and predicted wind speeds (F100), we can get an already good description of the future local wind speed.
- The location VE can be singled out from the others. Indeed the predicted wind speed at altitude 10m (F10) appears, and the forecasted wind speeds (F100 and F10) take longer to take over the in situ variables, especially when predicting wind power. This may be explained by a lesser representativity of the ECMWF forecasts for this location which may be linked to the elevation variations in the surroundings of the farm that we mentioned in Section 2.1.

As a concluding note, the dynamics of the local wind speed seem to be very well approximated by a simple linear model combining very few in situ variables and ECMWF ones. For predicting directly wind power however, we see in Section 5 the results are a bit less convincing, possibly due to the nonlinear aspect of the power curve.

4.2 Nonlinear variable selection with HSIC

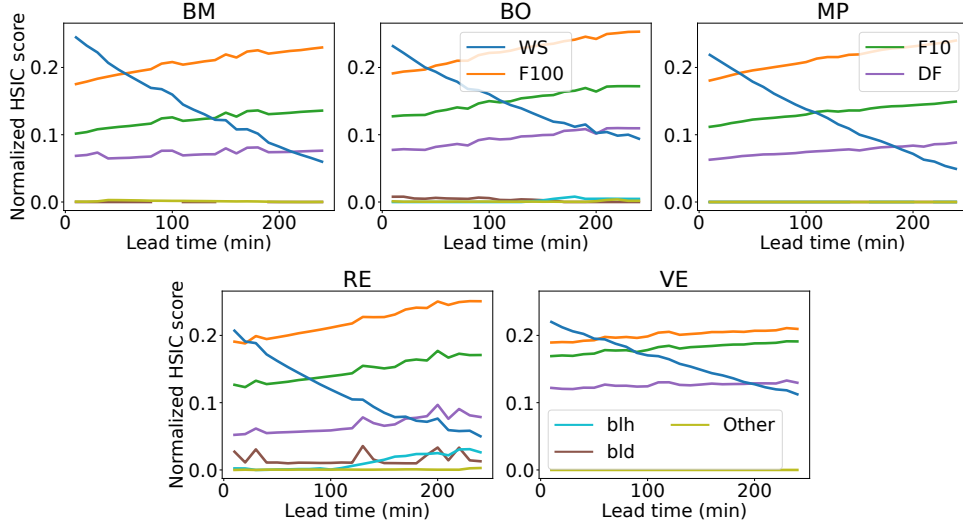


Figure 5: Nonlinear variable selection using HSIC (Wind speed as variable)

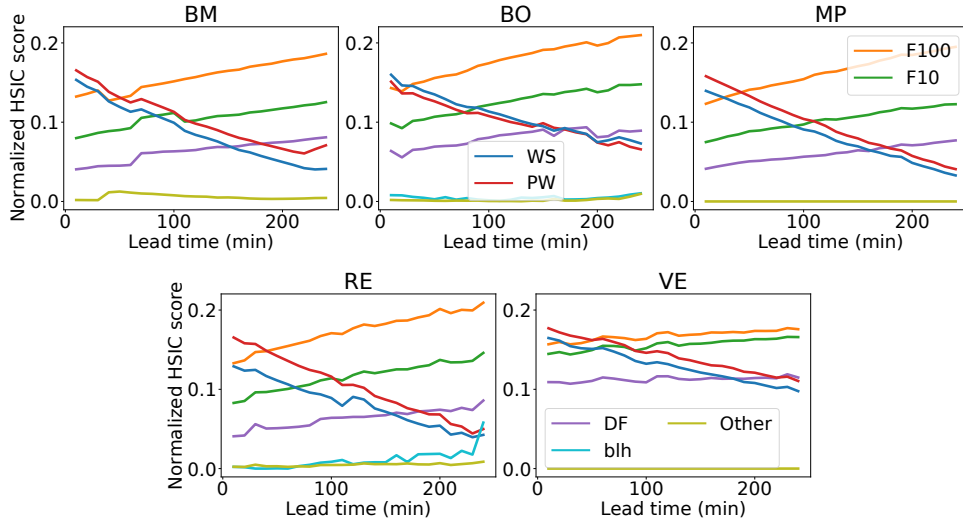


Figure 6: Nonlinear variable selection using HSIC (Wind power as target)

HSIC-score. For each farm and each split of the data we run BASHSIC on the training set until we have 5 variables left. Then for each variable we estimate the HSIC with that variable removed and normalize this value using the maximum HSIC value among these quantities. The normalized HSIC score appearing in the figures corresponds to 1 minus this score averaged over the training sets; the higher it is, the more important the variable is. We display the results in Figure 5 for wind speed and in Figure 6 for wind power.

Global interpretation. We make the following key observations:

- As expected, the in situ variables are most relevant for the shortest time horizon and the ECMWF variables take progressively the lead for longer horizons. However, compared to linear feature selection, ECMWF variables take the lead faster here—between 10-50 minutes as opposed to 70-100 minutes for linear selection. The retained variables are mostly the same as the one selected by the LASSO (WS or WS and PW depending on the target) and F100. However, F10 and DF are now more systemically retained with a significant importance.
- As for the LASSO selection, probably due to the lesser accuracy of ECMWF forecasts for this location, we can single out VE where the importance of the in situ variable(s) decreases much less fast than at the other farms.

Presence of DF and F10. In comparison with linear selection, we have two more variables of interest (DF and F10). F10 describes the wind speed at lower levels and DF the wind shear near the

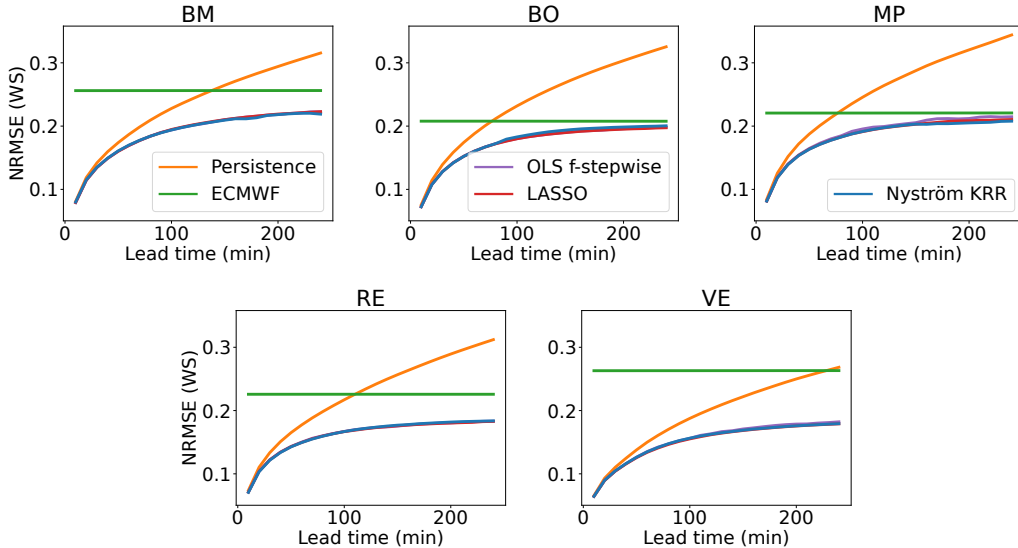


Figure 7: Average NRMSE at all time horizons for the three methods performing best overall according to Table 5.2 as well as for Persistence and ECMWF (wind speed as target)

surface. They thus bring useful information about the wind and its vertical shear, and likely help to correct deficiencies of the NWP model’s description of wind at 100m. The fact that they appear here and not in the linear framework indicates a nonlinear relation, which is not surprising as the shear relates to the level of turbulence in the boundary layer. Additionally, the above results bring a fairly sharp answer to another question underlying this study. As the calculation of near-surface winds in NWP models involves parameterizations, they are not the most reliable output of NWP models. Consequently, one could expect that, informed about other aspects of the boundary layer and local wind realizations, a nonlinear method could capture better the relationship between the boundary layer and the near-surface winds. This is not the case: BAHASIC clearly select rather the wind variables as the best source of information. Over variable terrain (VE), wind speed at different heights (F10) are more used, suggesting that the NWP model indeed fails to accurately describe the wind shear. And yet variables describing the boundary layer (e.g. stratification) still remain unused or marginal. Over flat terrain, the wind speed at 100m height (F100) is the major source of information, which is positive and encouraging regarding the accuracy of NWP models.

5 Wind speed and wind power forecasting

In this Section we compare several ML models for predicting both wind speed and wind power, exploiting the variable selection techniques from the previous section. We include the two main baselines, namely persistence which predicts the last in situ observation and ECMWF which uses the F100 forecasts from the ECMWF.

5.1 Experimental setup

Metrics. We evaluate our results using the normalized root mean squared error (NRMSE) as in [6]. Let $(z_t)_{t=1}^n$ denote the realizations of a (scalar-valued) target variable. We define its global mean as $\bar{z} = \frac{1}{n} \sum_{t=1}^n z_t$. Given a set of predicted values $(\hat{z}_t)_{t=1}^n$, it is defined as:

$$\text{NRMSE} := \frac{\sqrt{\frac{1}{n} \sum_{t=1}^n (\hat{z}_t - z_t)^2}}{\bar{z}}.$$

However, in order to compare the methods over the full time span, we need to introduce a new metric. If we were to simply average NRMSEs over time, then the resulting average would not make much sense because of the difference of magnitude between the errors at the different time horizons. Therefore, we propose to compare the NRMSE at each time horizon to a specific anchor reflecting what is achievable: the NRMSE of the best predictor for this time horizon. Let \mathcal{F} be a given set of predictors—for instance when predicting wind speed we have $\mathcal{F} := \{\text{Nyström KRR, LASSO, OLS f-stepwise, XG-Boost, Feedforward NN, Persistence, ECMWF}\}$. Given a predictor

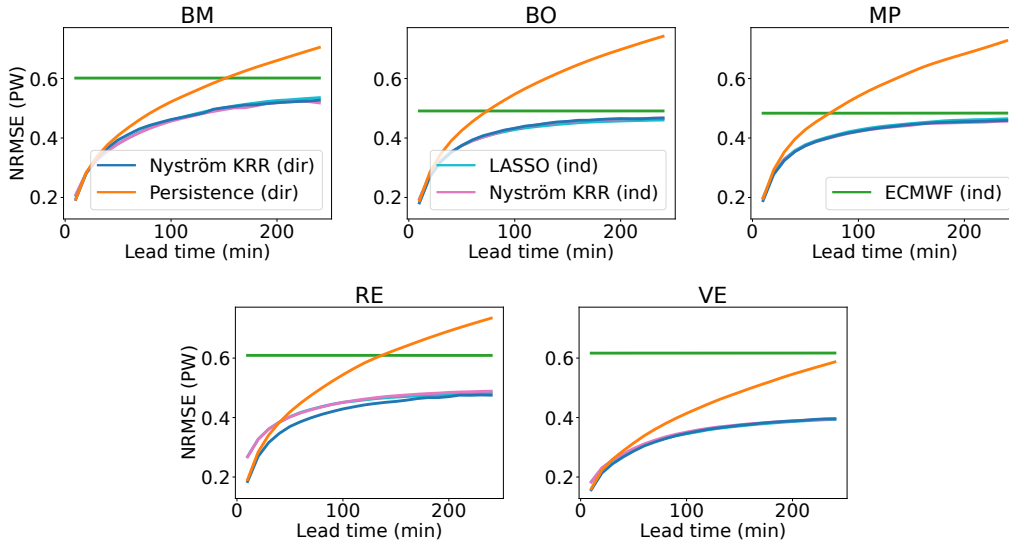


Figure 8: Average NRMSE at all time horizons for the three methods performing best overall according to Table 5.2 as well as for Persistence and ECMWF (wind power as target)

$f \in \mathcal{F}$, a prediction horizon $m_0 \in \llbracket m \rrbracket$ and a data split s (among a total of $S \in \mathbb{N}$ data splits), let $\text{NRMSE}_{s,m_0}^{(f)}$ denote the NRMSE of predictor f for the prediction horizon m_0 on the data split s . We then define the average NRMSE degradation of a predictor f_0 (with respect to the best predictor):

$$\frac{1}{mS} \sum_{s=1}^S \sum_{m_0=1}^m (\text{NRMSE}_{s,m_0}^{(f_0)} - \min_{f \in \mathcal{F}} \text{NRMSE}_{s,m_0}^{(f)}). \quad (5)$$

The best possible value is zero as it means that over all splits and over all horizons, the predictor was the best one.

Direct/indirect prediction. When we predict wind power, we consider two prediction techniques. Either we predict directly the wind power (direct approach) or we predict the wind speed which we transform using an estimated power curve in the same fashion as in [6] (indirect approach). A theoretical power curve could be used as well, however, in this work we estimate it from the training WS and PW observations using median of nearest neighbors interpolation using 250 neighbors.

Model selection. We follow the methodology introduced in Section 3.1 and refer the reader to Section 3.2 for details on the ML methods. In practice, for each data split, the key parameters of the different methods are chosen using the validation set (the regularization parameters λ , the Gaussian kernel’s γ for KRR, the number of variables for OLS f-stepwise, the architecture for the feedforward NN etc.). We provide the details of the considered parameters in the supplementary material.

5.2 Comparisons over the 10 minutes - 4 hours range

Method (average rank)	BM	BO	MP	RE	VE
LASSO (1.8)	1.12	0.13	0.16	0.14	0.16
Nyström KRR (2.0)	1.05	0.36	0.06	0.19	0.21
OLS f-stepwise (2.8)	1.1	0.16	0.47	0.18	0.34
Feedforward NN (3.4)	1.08	0.46	0.37	0.45	0.66
XG Boost (5.0)	1.81	1.25	1.63	0.74	0.97
ECMWF (6.4)	7.81	3.63	3.75	6.66	11.37
Persistence (6.6)	5.59	6.71	7.02	6.7	4.5

Table 4: Average NRMSE degradation w.r.t. best predictor for wind speed prediction ($\times 10^{-2}$)

Type	Method (average rank)	BM	BO	MP	RE	VE
Direct	Nyström KRR (2.4)	4.01	1.2	0.63	0.46	0.7
Indirect	Nyström KRR (3.0)	3.54	1.19	0.55	2.97	1.2
Indirect	LASSO (3.4)	4.04	0.8	1.08	2.72	0.87
Direct	Feedforward NN (4.0)	3.56	1.71	2.29	1.08	1.67
Indirect	OLS f-stepwise (4.4)	3.7	0.87	1.53	3.42	1.61
Direct	XG Boost (direct) (5.2)	4.62	2.39	1.5	1.8	1.8
Direct	OLS f-stepwise (6.6)	4.15	3.01	3.56	2.42	3.0
Direct	LASSO (direct) (7.0)	4.91	3.15	3.46	2.54	2.46
Direct	Persistence (9.4)	12.08	15.48	14.91	14.25	9.88
Indirect	ECMWF (10.2)	18.93	8.66	8.02	19.74	28.53
Indirect	Persistence (10.4)	13.21	15.89	15.22	16.39	10.86

Table 5: Average NRMSE degradation w.r.t. best predictor for wind power prediction ($\times 10^{-2}$)

Overall efficiency of ML models. From a general perspective, our experiments show that combining a NWP model’s outputs with local observations is very beneficial for predicting both wind speed and wind power at all the time horizons considered. To that end, Figure 5 displays the evolution of the NRSME for the two baselines (persistence and ECMWF) as well as for the three ML methods which performed best for wind speed prediction in Table 5.2 while Figure 5 displays the same for wind power prediction; the displayed ML methods being the top three ones from Table 5.2. For three farms (VE and to a lesser extend, BM and RE), even after four hours the improvement over ECMWF is still quite large. For BO and MP it becomes less important, yet still present. The improvement can be quite dramatic for very short horizons (first 100 minutes or so), and a bit less important for longer time horizons. This is probably linked to the representativity of the NWP model’s outputs which depends on the location.

Quantitative comparison. We now use the NRMSE degradation w.r.t. the best predictor (Equation 5) to compare the methods. The results are displayed in Table 5.2 (WS as target) and in Table 5.2 (PW as target). On the one hand, for wind speed prediction, the LASSO is the best ranked method. Relating this to the results from Section 4.1, it shows that the dynamics of the wind speed can be very well described by a linear combination of few ECMWF and local variables (essentially past local wind speeds and forecasted wind speeds). It suggests that the important nonlinear dynamics are overall well captured in the ECMWF variables. On the other hand, it seems better to predict directly wind power and do so using the Nyström KRR. This is not surprising, as the power curve is a nonlinear function and so we expected the linear methods to struggle in direct prediction. Moreover, in direct prediction, we implicitly include the power curve into the learning problem. This is advantageous since for instance a model trained to predict wind speed first will be very eager to forecast well high values (failing to do so would incur a high error term). However to predict wind power, producing accurate forecasts for higher wind speeds is less critical, since in the power curve, the actual wind power as a function of the wind speed is thresholded.

We note that the feedforward NN does not beat indirect prediction with the LASSO. This suggests that the higher expressiveness of NNs beyond the ability to infer the nonlinearity of the power curve is not needed. The difference of performance with direct Nyström KRR is imputable to the optimization error and variability implied by non-convexity of NNs whereas for Nyström KRR the optimization error is close to non-existent thanks to the closed-form solution. XG-Boost also does not perform well, this can be explained by the use of time series as features: these are very correlated and high dimensional which can make tree-based models unstable [11]. Doing some more work on feature pre-processing should improve the results.

5.3 Zoom on 10 minutes and 1 hour ahead forecasting

We now propose to zoom in on two time horizons of particular interest: 10 minutes and 1 hour ahead. We display the raw NRSMEs in Table 5.3 for WS and in Table 5.3 for PW.

For 10 minutes ahead prediction, persistence is unsurprisingly very efficient even though small yet significant improvements are already obtained by exploiting also ECMWF information with ML. For both the prediction of WS and PW, all three methods which beat persistence reach similar scores. For WS, these are the same as those performing best overall in Table 5.2: Nyström KRR, LASSO and OLS f-stepwise. However, for PW, these are Nyström KRR (direct), OLS f-stepwise

Horizon	Method (average rank)	BM	BO	MP	RE	VE
10 min	Nyström KRR (1.8)	8.0	7.25	8.15	7.08	6.44
	LASSO (2.0)	7.91	7.25	8.15	7.12	6.43
	OLS f-stepwise (2.2)	7.92	7.25	8.14	7.09	6.44
	Persistence (4.4)	8.11	7.55	8.43	7.39	6.56
	Feedforward NN (4.8)	8.26	7.55	8.33	7.37	6.8
	XG Boost (5.8)	8.72	8.26	9.57	7.61	6.77
	ECMWF (7.0)	25.61	20.78	22.06	22.57	26.3
1 hour	Nyström KRR (1.6)	17.01	16.03	17.11	14.94	13.48
	LASSO (1.8)	16.94	16.04	17.13	14.95	13.4
	OLS f-stepwise (2.6)	16.92	16.06	17.3	15.02	13.52
	Feedforward NN (4.0)	17.27	16.27	17.32	15.17	13.72
	XG Boost (5.0)	17.69	17.19	18.77	15.66	14.16
	Persistence (6.0)	18.68	18.81	20.09	17.73	15.0
	ECMWF (7.0)	25.61	20.78	22.06	22.58	26.3

Table 6: Average NRMSE for 10 minutes and 1 hour ahead wind speed prediction ($\times 10^{-2}$)

(direct), LASSO (direct). The first is the leading method in Table 5.2, but the other two are not. We explained their poor performance by the nonlinearity of the power curve which they cannot capture. Nevertheless for the very short-term, this is not an issue. This confirms our findings from Section 4: for 10 minutes ahead prediction, the last observed wind power is the most crucial information.

For 1 hour ahead prediction, the rankings of ML methods for both wind speed (Table 5.3) and wind power (Table 5.3) almost perfectly match the rankings of methods on the whole time span (Table 5.2 for WS and Table 5.2 for PW).

Overall, this analysis confirms that for both the very short term and the longer term Nyström KRR is a safe choice for wind speed and wind power prediction. For the latter the direct approach with this method should be preferred.

5.4 Computational times

We now address the practical concern of computational times. To that end, we measure the time on a laptop to fit the different procedures and to produce the corresponding forecasts. We do so only for one wind farm (BO). We draw randomly 50 pairs containing a split from the dataset (see Section 2.2) and a parameter configuration among the ones we used. Then we time the procedures using these pairs. We display the median as well as the 10% and 90% quantiles of the obtained computational times in Table 5.4. To put these computational times into perspective, on the one hand the regression models have extra parameters to tune, and therefore many configurations must be tested. On the other hand Nyström BAHASIC seems expensive but no such tuning must be performed (it eliminates the variables gradually, therefore the ranking can be used to include more or less features afterwards).

6 Conclusion

We showed through experiments on several wind farms that we can improve very significantly short-term local forecasts of both wind speed and wind power by combining statistically a NWP model’s outputs with local observations. To better understand how, we studied in details the evolution of the variables’ importance using two metrics, a linear one based on LASSO coefficients and a nonlinear one using HSIC. Our global conclusion is that NWP wind variables are a very relevant source of information to complement local observations, even for the very short-term. To forecast wind speed, a parsimonious linear combination of NWP and local variables (with the LASSO) yielded the best result. While to forecast wind power, direct prediction (no power curve involved) with a nonlinear method (Nyström KRR) using a few variables (selected with BAHASIC) is preferable. Beyond the ability to capture the nonlinearity of the power curve, it seems unnecessary to use more complex models which hints that NWP model’s outputs describe sufficiently the other nonlinear dynamics involved. For future work, assessing the variability of the predictions, for instance by predicting conditional quantiles [20] which would inform us on the expected distribution of the predictions. This could help mitigate the intermittent effects of wind power production further.

Horizon	Type	Method (average rank)	BM	BO	MP	RE	VE
10 min	Direct	Nyström KRR(1.4)	19.36	18.16	18.94	18.49	15.7
	Direct	OLS f-stepwise (2.0)	19.04	18.2	18.96	18.53	15.8
	Direct	LASSO (2.6)	19.06	18.22	19.01	18.56	15.78
	Direct	Persistence (4.4)	19.44	18.92	19.63	19.13	16.09
	Direct	Feedforward NN (4.6)	19.73	18.81	19.56	19.3	16.3
	Direct	XG Boost (6.0)	19.9	19.41	19.77	19.38	16.59
	Indirect	LASSO (7.6)	20.73	19.48	19.91	26.84	18.34
	Indirect	Nyström KRR (8.0)	20.86	19.51	19.87	26.8	18.36
	Indirect	OLS f-stepwise (8.4)	20.73	19.48	19.89	26.87	18.39
	Indirect	Persistence (10.0)	21.67	20.41	20.77	27.32	18.8
	Indirect	ECMWF (11.0)	60.15	49.09	48.34	60.91	61.66
1 hour	Indirect	Nyström KRR (2.8)	40.02	39.04	38.74	41.53	31.15
	Direct	Nyström KRR (3.0)	41.26	39.36	38.85	38.59	30.46
	Indirect	LASSO (3.4)	40.11	39.07	39.1	41.72	30.8
	Indirect	OLS f-stepwise (4.6)	39.97	39.16	39.37	42.2	31.36
	Direct	Feedforward NN (4.8)	40.51	39.64	39.58	39.44	31.16
	Direct	LASSO (5.2)	40.39	39.93	40.06	39.83	31.07
	Direct	OLS f-stepwise (5.6)	40.37	39.82	40.26	39.67	31.53
	Direct	XG Boost (6.6)	41.89	40.43	39.22	39.99	31.81
	Direct	Persistence (9.0)	43.58	45.52	45.44	44.84	33.88
	Indirect	Persistence (10.0)	44.68	46.01	45.99	47.36	35.08
	Indirect	ECMWF (11.0)	60.15	49.1	48.34	60.91	61.67

Table 7: Average NRMSE for 10 minutes and 1 hour ahead wind power prediction ($\times 10^{-2}$)

Task	Method	Fit time (s)	Predict time (s)
Selection	Nyström BAHSIC	74.61 (73.38, 89.00)	-
Selection & regression	LASSO	1.39 (0.01, 5.03)	0.039 (0.036, 0.044)
Selection & regression	OLS f-stepwise	3.58 (2.92, 4.30)	0.037 (0.037, 0.043)
Regression	Nyström KRR	0.451 (0.414, 0.563)	0.332 (0.300, 0.433)
Regression	XgBoost	0.450 (0.405, 0.548)	0.058 (0.053, 0.070)
Regression	Feedforward NN	75.84 (72.70, 77.27)	0.029 (0.028, 0.031)

Table 8: Median (10 % quantile, 90 % quantile) of fit and predict computational times on laptop for direct wind power prediction on BO farm.

Acknowledgments

This work received support from the Télécom Paris research chair on Data Science and Artificial Intelligence for Digitalized Industry and Services (DSADIS). It was conducted as part of the Energy4Climate Interdisciplinary Center (E4C) of Institut Polytechnique de Paris and Ecole des Ponts ParisTech. It has received support as well from the 3rd Programme d’Investissements d’Avenir [ANR-18-EUR-0006-02] and from the Foundation of Ecole polytechnique (Chaire “Défis Technologiques pour une Énergie Responsable”). The authors would like to thank the company Zéphyr ENR, and especially its CEO Christian Briard, for providing the data from its wind farms.

References

- [1] J.A. Baars and C.F. Mass. Performance of National Weather Service forecasts compared to operational, consensus and weighted model output statistics. *Wea. Forecast.*, 20:1034–1047, 2005.
- [2] P. Bauer, A. Thorpe, and G. Brunet. The quiet revolution of numerical weather prediction. *Nature*, 525:47–55, 2015.
- [3] Amir Beck and Marc Teboulle. A fast iterative shrinkage-thresholding algorithm for linear inverse problems. *SIAM Journal on Imaging Sciences*, 2(1):183–202, 2009.

- [4] Tianqi Chen and Carlos Guestrin. Xgboost: A scalable tree boosting system. In *Proceedings of the 22nd ACM SIGKDD International Conference on Knowledge Discovery and Data Mining*, pages 785–794, 2016.
- [5] Petros Drineas and Michael Mahoney W. On the nystrom method for approximating a gram matrix for improved kernel-based learning. *Journal of Machine Learning Research*, 6:2153–2175, 2005.
- [6] Aurore Dupré, Philippe Drobinski, Bastien Alonzo, Jordi Badosa, Christian Briard, and Riwal Plougonven. Sub-hourly forecasting of wind speed and wind energy. *Renewable Energy*, 145: 2373–2379, 2020.
- [7] Aurore Dupré, Philippe Drobinski, Jordi Badosa, Christian Briard, and Peter Tankov. The economic value of wind energy nowcasting. *Energies*, 13(20):5266, 2020.
- [8] Jerome H. Friedman. Greedy function approximation: A gradient boosting machine. *The Annals of Statistics*, 29(5):1189 – 1232, 2001.
- [9] H.R. Glahn and D.A. Lowry. The use of model output statistics (MOS) in objective weather forecasting. *J. App. Meteor.*, 11:1203–1211, 1972.
- [10] N. Goutham, B. Alonzo, A. Dupré, R. Plougonven, R. Doctors, L. Liao, M. Mougeot, A; Fischer, and P. Drobinski. Using machine-learning methods to improve surface wind speed from the outputs of a numerical weather prediction model. *Boundary Layer Meteorology*, 2021.
- [11] Baptiste Gregorutti, Bertrand Michel, and Philippe Saint-Pierre. Correlation and variable importance in random forests. *Statistics and Computing*, 27:659–678, 2017.
- [12] Arthur Gretton, Olivier Bousquet, Alex Smola, and Bernhard Schölkopf. Measuring statistical dependence with hilbert-schmidt norms. In *Algorithmic Learning Theory*, pages 63–77. Springer Berlin Heidelberg, 2005.
- [13] Arthur Gretton, Kenji Fukumizu, Choon Teo, Le Song, Bernhard Schölkopf, and Alex Smola. A kernel statistical test of independence. In *Advances in Neural Information Processing Systems (NIPS)*, volume 20, 2008.
- [14] Yan Han, Lihua Mi, Lian Shen, C.S. Cai, Yuchen Liu, Kai Li, and Guoji Xu. A short-term wind speed prediction method utilizing novel hybrid deep learning algorithms to correct numerical weather forecasting. *Applied Energy*, 312, 2022.
- [15] Trevor Hastie, Jerome H. Friedman, and Robert Tibshirani. *The Elements of Statistical Learning*. Springer, 2001.
- [16] Victoria Hoolohan, Alison S. Tomlin, and Timothy Cockerill. Improved near surface wind speed predictions using gaussian process regression combined with numerical weather predictions and observed meteorological data. *Renewable Energy*, 126:1043–1054, 2018.
- [17] IEA. Renewables information. *International Energy Agency*, page 12, 2018.
- [18] IEA. Renewables: Analysis and forecast to 2026. *International Energy Agency*, page 175, 2021.
- [19] Eugenia Kalnay. *Atmospheric modeling, data assimilation and predictability*. Cambridge University Press, 2003.
- [20] Roger Koenker and Kevin F. Hallock. Quantile regression. *Journal of Economic Perspectives*, 15(4):143–156, December 2001.
- [21] Hui Liu, Chao Chen, Xinwei Lv, Xing Wu, and Min Liu. Deterministic wind energy forecasting: A review of intelligent predictors and auxiliary methods. *Energy Conversion and Management*, 195:328–345, September 2019.

- [22] V. Masson-Delmotte, P. Zhai, A. Pirani, S.L. Connors, C. Péan, S. Berger, N. Caud, Y. Chen, L. Goldfarb, M. I. Gomis, M. Huang, K. Leitzell, E. Lonnoy, J.B.R. Matthews, T. K. Maycock, T. Waterfield, O. Yelekçi, R. Yu, and B. Zhou (eds.). IPCC, 2021: Summary for Policymakers. In *Climate Change 2021: The Physical Science Basis. Contribution of Working Group I to the Sixth Assessment Report of the Intergovernmental Panel on Climate Change*, pages 1–42, 2021.
- [23] Inci Okumus and Ali Dinler. Current status of wind energy forecasting and a hybrid method for hourly predictions. *Energy Conversion and Management*, 123:362–371, September 2016.
- [24] Fabian Pedregosa, Gaël Varoquaux, Alexandre Gramfort, Vincent Michel, Bertrand Thirion, Olivier Grisel, Mathieu Blondel, Peter Prettenhofer, Ron Weiss, Vincent Dubourg, et al. Scikit-learn: Machine learning in python. *Journal of machine learning research*, 12(Oct):2825–2830, 2011.
- [25] Alessandro Rudi, Raffaello Camoriano, and Lorenzo Rosasco. Less is more: Nyström computational regularization. In *Advances in Neural Information Processing Systems (NIPS)*, pages 1657–1665, 2015.
- [26] Bernhard Schölkopf and Alexander J. Smola. *Learning with Kernels: Support Vector Machines, Regularization, Optimization, and Beyond*. The MIT Press, 2002.
- [27] John Shawe-Taylor and Nello Cristianini. *Kernel Methods for Pattern Analysis*. Cambridge University Press, 2004.
- [28] Le Song, Alex Smola, Arthur Gretton, Justin Bedo, and Karsten Borgwardt. Feature selection via dependence maximization. *Journal of Machine Learning Research*, 13:1393–1434, 2012.
- [29] A. Tascikaraoglu and M. Uzunoglu. A review of combined approaches for prediction of short-term wind speed and power. *Renewable and Sustainable Energy Reviews*, 34:243–254, 2014.
- [30] Robert Tibshirani. Regression shrinkage and selection via the lasso. *Journal of the Royal Statistical Society. Series B (Methodological)*, 58(1):267–288, 1996.
- [31] Christopher Williams and Matthias Seeger. Using the nyström method to speed up kernel machines. In *Advances in Neural Information Processing Systems (NIPS)*, volume 13, 2001.
- [32] L.J. Wilson and M. Vallée. The Canadian Updateable Model Output Statistics (UMOS) system: Design and Development tests. *Wea. Forecast.*, 17:206–222, 2002.
- [33] Tianbao Yang, Yu-feng Li, Mehrdad Mahdavi, Rong Jin, and Zhi-Hua Zhou. Nyström method vs random fourier features: A theoretical and empirical comparison. In F. Pereira, C.J. Burges, L. Bottou, and K.Q. Weinberger, editors, *Advances in Neural Information Processing Systems (NIPS)*, volume 25. Curran Associates, Inc., 2012.
- [34] M. Zamo, L. Bel, O. Mestre, and J. Stein. Improved gridded wind speed forecasts by statistical postprocessing of numerical models with block regression. *Weather and Forecasting*, 31:1929–1945, 2016.
- [35] Qinyi Zhang, Sarah Filippi, Arthur Gretton, and Dino Sejdinovic. Large-scale kernel methods for independence testing. *Statistics and Computing*, 28, 2018.

Experimental details

This short appendix is dedicated to the full description of the parameters that we use in the experiments.

A Importance of variables and their evolution through time

A.1 LASSO

The main parameter of the LASSO is the regularization intensity λ . For each data split, we select it based on the NRMSE achieved on the validation set. We consider values in a geometric grid of size 30 ranging from 10^{-5} to 1.

A.2 BAHSIC

We use a Gaussian kernel for both for the input kernel and the output one:

$$k_\gamma(\mathbf{z}, \mathbf{z}') := \exp(-\gamma(\|\mathbf{z} - \mathbf{z}'\|_2^2)).$$

We follow [28] in the choice of the parameter γ . We standardized both our input and output data so we can apply their heuristic: set this parameter to $\frac{1}{2d}$ where d is the dimension of the inputs of the kernel. Then for the input kernel we have $d = q$ and for the output one $d = m$.

For the Nyström approximation, we use fewer points than for the KRR since as highlighted in [35], for detection of dependency, a fewer number of anchor points are generally sufficient. We then use 100 points for both the input and output approximation.

B Wind speed and wind power forecasting

As a first general note, since we standardized all the variables, we consider the same parameter ranges for prediction of wind speed and wind power.

LASSO The fitted models used for interpretation in the variable selection section are the same that we use here (so the considered parameters are the same).

OLS f-stagewise We selected on the validation set the number of included variables. We consider the following number of variables: $\{5, 6, 7, 8, 9, 10, 11, 12, 13, 14, 15, 20\}$.

Nyström KRR We select both the input Gaussian kernel's γ parameter and the regularization parameter λ . We consider the following values:

- γ in a geometric space of length 30 ranging from 10^{-6} to 10^{-3} .
- λ in a geometric space of length 30 ranging from 10^{-4} to 5.

For the Nyström approximation, we use 300 sampled points.

Xg-Boost For Xg-Boost, we validate the trees' maximum depth considering values in $\{3, 4, 5, 6\}$ as well as the minimum loss reduction parameter for values in a geometric space of size 50 ranging from 10^{-7} to 50.

Feedforward NN We consider a NN with 3 hidden layers and validate the number of neurons per layer choosing among the possible values $\{(35, 20, 5), (50, 25, 10), (50, 35, 20), (75, 50, 25)\}$.